Bioorganic & Medicinal Chemistry Letters 24 (2014) 1784–1789

Contents lists available at ScienceDirect

Bioorganic & Medicinal Chemistry Letters

journal homepage: www.elsevier.com/locate/bmcl

Synthesis and evaluation of carbon-linked analogs of dual orexin receptor antagonist filorexant

Scott D. Kuduk [a,*], Jason W. Skudlarek [a], Christina N. Di Marco [a], Joseph G. Bruno [b], Mark A. Pausch [b], Julie A. O'Brien [b], Tamara D. Cabalu [c], Joanne Stevens [d], Joseph Brunner [d], Pamela L. Tannenbaum [d], Anthony L. Gotter [e], Christopher J. Winrow [e], John J. Renger [e], Paul J. Coleman [a]

[a] Department of Medicinal Chemistry, Merck Research Laboratories, West Point, PA 19486, USA
[b] Department of In Vitro Pharmacology, Merck Research Laboratories, West Point, PA 19486, USA
[c] Department of Drug Metabolism, Merck Research Laboratories, West Point, PA 19486, USA
[d] Department of In Vivo Pharmacology, Merck Research Laboratories, West Point, PA 19486, USA
[e] Department of Neuroscience, Merck Research Laboratories, West Point, PA 19486, USA

ARTICLE INFO

Article history:
Received 18 January 2014
Revised 7 February 2014
Accepted 10 February 2014
Available online 19 February 2014

Keywords:
Orexin
Insomnia
Antagonist

ABSTRACT

Analogs of the dual orexin receptor antagonist filorexant were prepared. Replacement of the ether linkage proved highly sensitive toward modification with an acetylene linkage providing compounds with the best in vitro and in vivo potency profiles.

The orexin neuropeptides and their receptors have a demonstrated role in regulating sleep/wake state and recent research has generated significant interest in targeting the orexin receptors for related disorders. The characterization of a novel neuropeptide secreted from the hypothalamus, naming the peptide hypocretin[1] and orexin,[2] was achieved via genetic and biochemical approaches, with the orexin naming most frequently utilized.[3] Orexin neuropeptides (OX-A and OX-B) are derived from orexinergic neurons localized in the lateral hypothalamus, and signal through two G-protein coupled receptors (GPCR's), Orexin Receptor 1 (OX_1R) and Orexin Receptor 2 (OX_2R).[3]

These receptors are disseminated in key brain regions responsible for governing wake, vigilance and reward seeking behaviors. Orexin signaling is most active during the normal wake period and falls silent during the sleep period.[4–6] Several companies have identified dual orexin receptor antagonists (DORAs) targeting both OX_1R and OX_2R, or selective orexin receptor antagonists (SORAs), and many have advanced through late stage clinical development.[7–10] Numerous reviews are available in this context.[11–14]

Two DORAs, suvorexant and filorexant, have been discovered and advanced into clinical development at Merck (Fig. 1). Filorexant was most recently described as a potent DORA that is efficacious in promoting sleep in rats and dogs, and has been reported to be in Phase II trials. Limited SAR data has been reported for filorexant, mostly to the carboxamide and fluoro-pyridine regions of the molecule.[15] In this Letter, we describe SAR analysis of the role of the ether linkage between the piperidine central ring

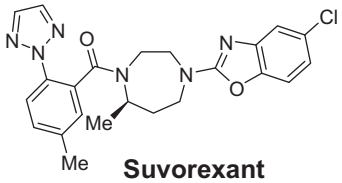

Suvorexant

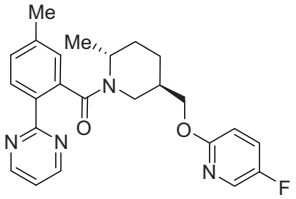

Filorexant

Figure 1.

* Corresponding author. Tel.: +1 215 652 5147; fax: +1 215 652 3971.
E-mail address: scott_d_kuduk@merck.com (S.D. Kuduk).

http://dx.doi.org/10.1016/j.bmcl.2014.02.026
0960-894X/

and the fluoropyridine, with an emphasis of all carbon linkages (ethyl) with varied degrees of flexibility (sp3, sp2, and sp hybridization).

The synthetic route used to access carbon-linked target molecules is shown in Schemes 1–3. Coupling of triazole carboxylic acid **6** and piperidinol **7** was mediated by EDC followed by

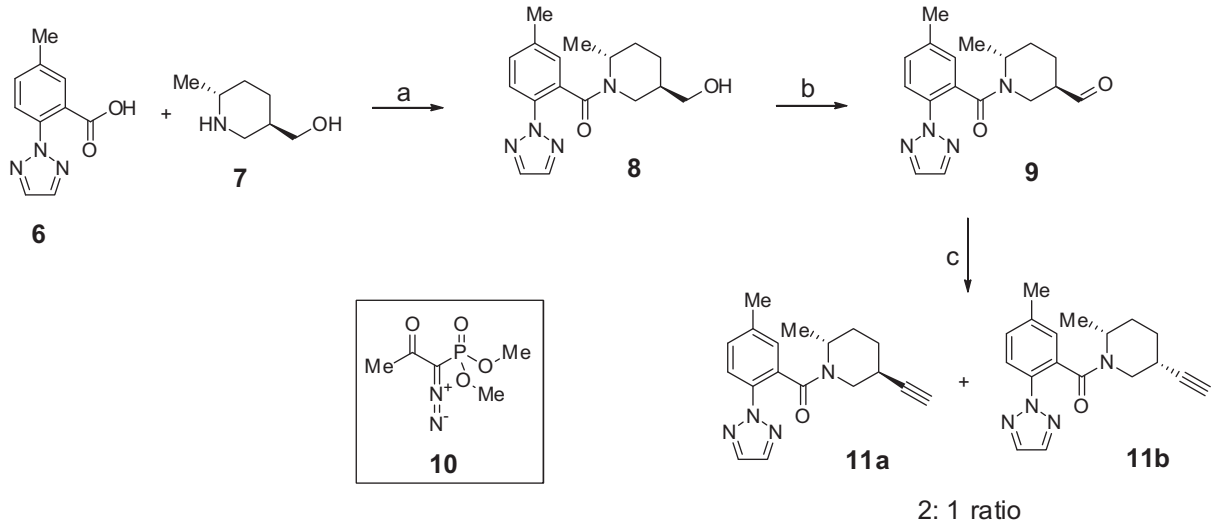

Scheme 1. (a) EDC, HOBt, Hunig's base, DMF. (b) Diacetoxyiodobenzene, TEMPO, CH_2Cl_2. (c) Potassium carbonate, 10, MeOH.

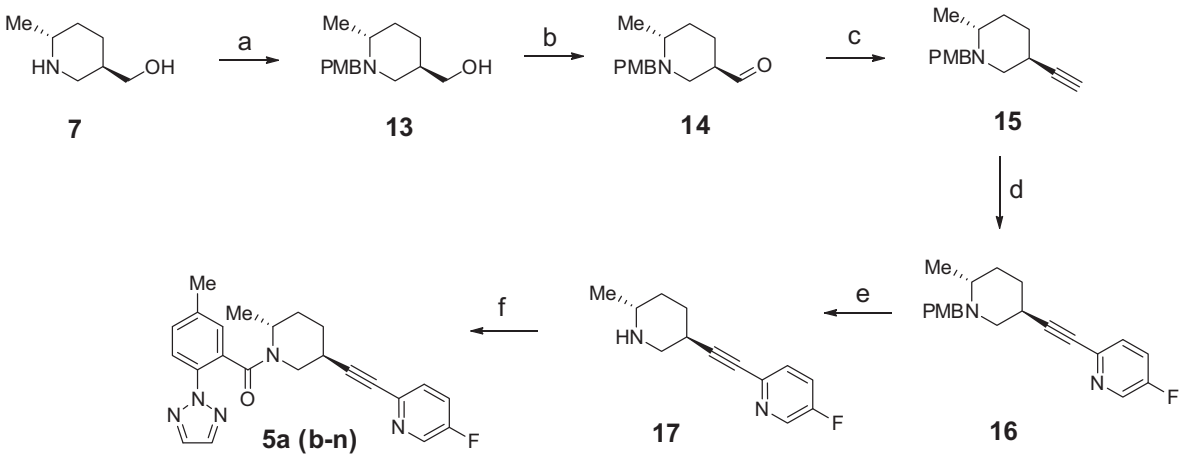

Scheme 2. (a) *p*-Anisaldehyde, $NaBH_3CN$, MeOH. (b) Oxalyl chloride, DMSO, Et_3N, CH_2Cl_2. (c) Potassium carbonate, 10. (d) 2-Bromo-5-fluoropyridine, $Pd(PPh_3P)_4$, CuI, Et_3N. (e) (1) 1-Chloroethyl chloroformate, Et_3N, CH_2Cl_2; (2) MeOH, reflux. (f) EDC, HOAt, Hunig's base, DMF.

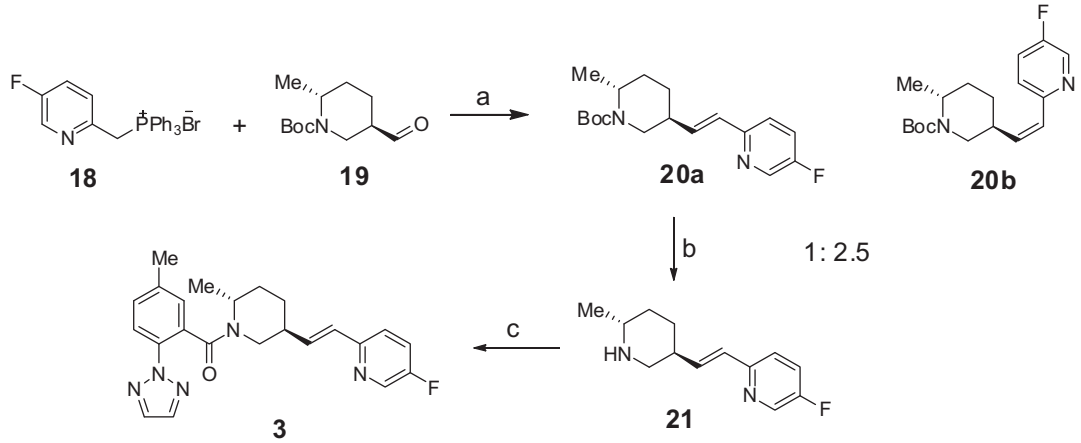

Scheme 3. (a) NaH, THF, 0 °C-rt. (b) HCl, dioxane. (C) 6, EDC, HOAt, Hunig's base.

oxidation of the alcohol to provide aldehyde **9**.[16] Alkynylation using the Bestmann reagent **10**[17] provided alkynes **11a** and **11b**, albeit in an undesirable 2:1 ratio of *cis*/*trans* isomers due to epimerization of the aldehyde under the reaction conditions. The aldehyde group in **9** is likely sensitive to epimerization due to being in a pseudo-axial position due to the 1,3-allylic strain imposed by the 2-methyl group and the arylcarboxamide.[15]

In order to circumvent this issue, an alternate protecting group strategy was investigated that would avoid the 1,3-allylic strain and bias both the 2- and 5-substituents in the equatorial position to avoid epimerization. Toward this end, piperidinol **7** underwent reductive amination with *para*-anisaldehyde to provide PMB protected alcohol **13**. Oxidation, followed by alkynylation provided **15** as a single *trans* isomer. Sonogashira cross-coupling with 2-iodo-4-fluoropyridine provided **16**. Subsequent removal of the PMB group and amide coupling provided alkyne **5a**. Analogs of **5a** were prepared via this route using different aryl iodides or bromides in with **15**. Hydrogenation of **5a** with Pd/C in MeOH generated ethyl linked analog **2** while Lindlar reduction provided *cis*-olefin **4** (not shown).

Lastly, Wittig olefination with phosphonium salt **18** and aldehyde **19** provided **20a** and **20b**, as a separable mixture, in a ratio of 1:2.5. Removal of the protecting group in **20a** was followed by coupling with acid **6** to deliver *trans*-olefin linker analog **3**.

Having prepared the targeted new carbon-carbon linker modified analogs, evaluation in primary in vitro assays was conducted. Compounds were evaluated for OX_2R and OX_1R potency through an in vitro radioligand binding assay to membranes from human cells overexpressing the orexin receptor and reported as K_i. In addition, a cell-based functional FLIPR (fluorometric imaging plate reader) assay in which Ca^{2+} flux is measured as a functional determinant of orexin binding, was also conducted.[18] Results for compounds **1**–**5a** are shown in Figure 2.

Relative to potent DORA comparator **1** containing the ether linkage found in filorexant, the direct oxygen for methylene replacement in the form of ethyl analog **2** lost considerable affinity in the binding assay (>10×) and potency in the functional assay, highlighting a key role for the oxygen heteroatom. The effect was more pronounced for OX_1R in both assays. The *trans*-olefin **3** retained considerably more potency at OX_2R in the functional assay with an IC_{50} = 34 nM, but with an ~8-fold decrease at OX_1R, similar to that seen with ethyl **2**. The corresponding *cis*-olefin linkage **4** was less effective than the *trans* providing binding and FLIPR data similar to that for ethyl compound **2**. Lastly, alkyne **5a** provided very high binding affinity at both sub-types (K_i = 1.1 nM) and potent functional activity at OX_2R (IC_{50} = 24 nM) and OX_1R (IC_{50} = 31 nM). Based on this promising potency and dual activity profile, additional SAR evaluation was conducted with the alkyne moiety in place.

In order to more fully scope out the SAR using the new alkynyl modification, examination of the role of the pyridine ring and substituents was investigated as shown in Table 1. Removal of the fluorine atom (**5b**) led to a 2-3-fold loss in functional activity, but a more pronounced effect (~10×) was noted in the binding assay. Pyridine isomer **5c** lost considerable binding affinity relative to **5b**, while 4-pyridyl **5d** proved similar.

Alkyne **5a** was highly lipophilic (HPLC log$D$ = 3.7)[19] so additional polar substituents on the pyridine such as hydroxyl groups were investigated. Hydroxy pyridine **5e** provided balanced binding affinity at both receptor sub-types (K_i = 24 nM), while isomer **5f** showed preferred binding at OX_2R over OX_1R (K_i's = 7.5 and 866 nM, respectively), and this preference was noted in the

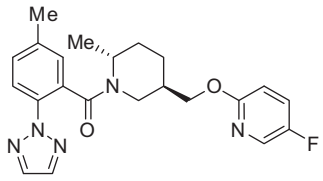

1
hOX2R K_i = 0.2 nM
hOX1R K_i = 1 nM
hOX2R IC_{50} = 15 nM
hOX1R IC_{50} = 16 nM

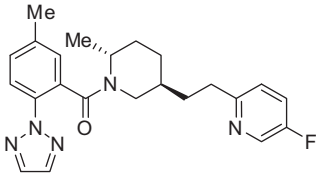

2
hOX2R K_i = 26 nM
hOX1R K_i = 470 nM
hOX2R IC_{50} = 145 nM
hOX1R IC_{50} = 861 nM

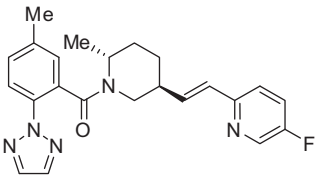

3
hOX2R K_i = 3.0 nM
hOX1R K_i = 17 nM
hOX2R IC_{50} = 34 nM
hOX1R IC_{50} = 140 nM

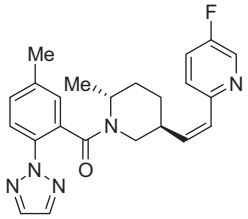

4
hOX2R K_i = 28 nM
hOX1R K_i = 135 nM
hOX2R IC_{50} = 417 nM
hOX1R IC_{50} = 706 nM

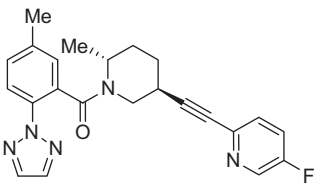

5a
hOX2R K_i = 1.1 nM
hOX1R K_i = 1.1 nM
hOX2R IC_{50} = 24 nM
hOX1R IC_{50} = 31 nM

Figure 2.

Table 1

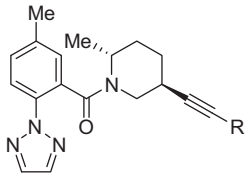

L#	R	OX2R BIND[a]	OX1R BIND[a]	OX2R FLIPR[a]	OX1R FLIPR[a]
5a	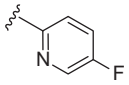	1.1	1.1	24	31
5b		11	27	42	100
5c		41	107	28	83
5d	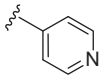	7.0	26	nd	nd
5e	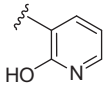	24	24	nd	nd
5f	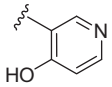	7.5	866	52	3878
5g	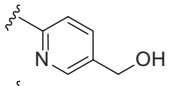	130	211	nd	nd
5h	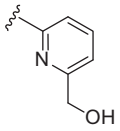	5.6	18	26	59
5i	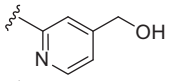	42	76	nd	nd
5j	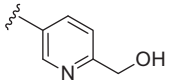	~150	339	nd	nd
5k	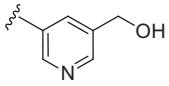	32	108	nd	nd
5l	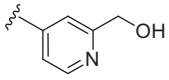	25	75	100	298
5m	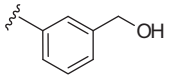	0.53	0.56	6.3	6.3

[a] Values represent the average of $n \geqslant 2$ experiments.

functional assay as well. Adding a hydroxy methyl group on the 2-pyridyl was examined (**5g–i**) and SAR indicated the position of the group significantly affected the binding affinity. Analog **5h** with the hydroxymethyl at the 3-position was most tolerant in terms of binding with a ~5–15 fold decrease, while functional potency (OX_2R IC_{50} = 26 nM, OX_1R IC_{50} = 59 nM) was similar to parent alkyne **5a**. The 3-hydroxymethyl analogs in the context of the 3-pyridine (**5j**,**k**) showed weaker binding affinity than the 2-pyridyl counterpart **5i**. Also, the 4-pyridyl-3-hydroxymethyl **5l** was substantially weaker in binding and FLIPR. Lastly, a 3-hydroxylmethyl analog with the pyridine nitrogen absent in the form of phenyl analog **5m** was also evaluated. This compound proved to be a very potent DORA in the FLIPR assay (OXR IC_{50} = 6.3 nM) with highest affinity (OX_2R K_i = 0.53 nM, OX_1R K_i = 0.56 nM) of any analog prepared, but was also an inhibitor of CYP3A4 (IC_{50} ~4 uM).

While hydroxymethylpyridine **5h** did have the desirable effect of decreasing the lipophilicity (HPLC log*D* = 2.1), and maintained good functional potency relative to **5a**, it proved to be a substrate for the CNS efflux transporter P-glycoprotein (P-gp).[20] Fluoropyridine **5a** gave the best overall profile in terms of binding, functional potency, and P-gp properties (Fig. 3). Accordingly, more advanced characterization was conducted to see if advantages could be realized over 5-ether linked DORAs.

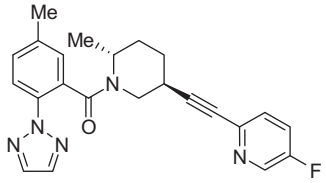

5a

HPLC logD = 3.7
HPLC sol (pH 7) = 124 μM
PPB = 99.1 (h), 96.1 (d)
Dog IV PK: Cl = 1.6 mL/min/kg,
Vdss = 0.26, $t_{1/2}$ = 2.0 h
hERG = 23 μM
CYP inhibition: 3A4 > 50 μM,
2C9: 32 μM, CYP2D6 > 50 μM

Figure 3.

To evaluate its in vivo pharmacodynamics and selectivity, DORA **5a** was examined in a mouse sleep model (Fig. 4). Both wild type and OX_2R knock-out mice surgically implanted with radio telemetry transmitters measuring electroencephalography (EEG) and electromyogram (EMG) activity to determine vigilance state over time as previously described.[22] In wildtype mice compound **5a** dosed orally at 100 mg/kg promoted sleep with sleep stage architecture consistent with other orexin receptor antagonists across species.[21,22] Significant active wake reduction was observed for 2 h following treatment accompanied by corresponding increases in delta and REM sleep. These responses are qualitatively similar to that induced by DORA-22, an analog of filorexant evaluated in mice, where active wake reductions are accompanied by proportionally similar slow wave sleep and REM increases.[22] While compound **5a**, promotes sleep to a similar magnitude as DORA-22, its effects are more rapid and brief; it attenuates active wake and increases REM and delta sleep to a greater extent during the first 30 min after treatment relative to DORA-22 used at the same dose (100 mg/kg), and the duration of sleep promoting effects are shorter, lasting for 2 h relative to 4 h induced by DORA-22.[22] Notably, the sleep promoting effects of compound **5a** were largely

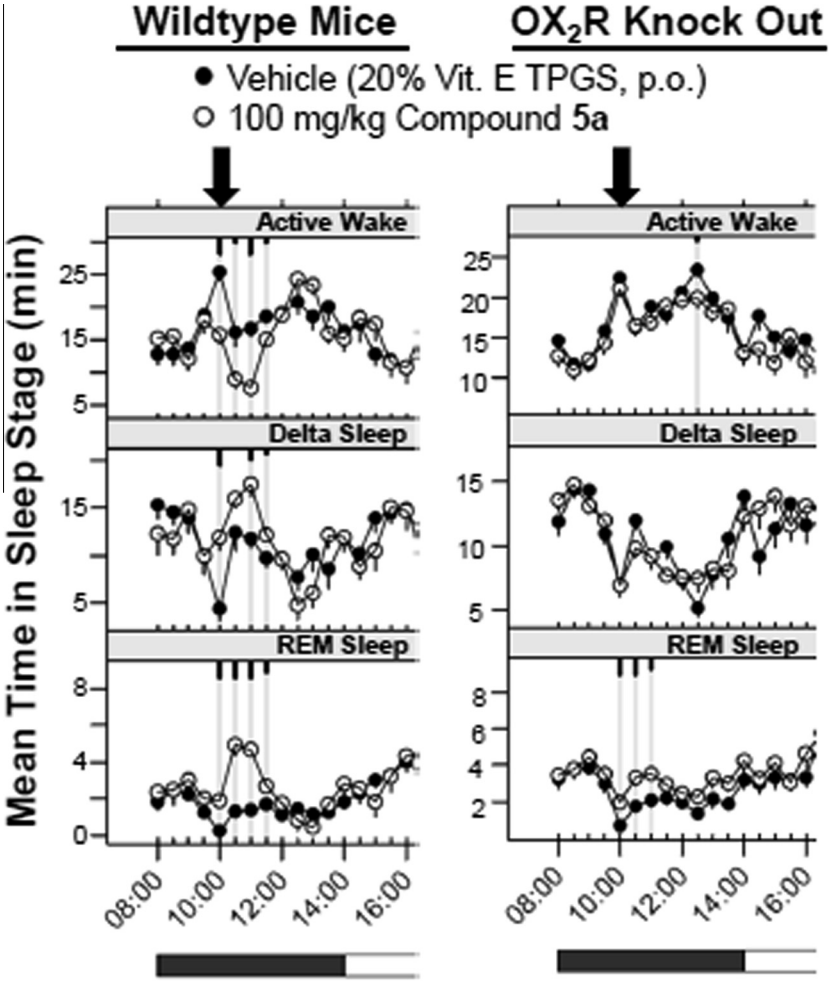

Figure 4. Sleep promoting responses to compound **5a** are largely due to activity at OX_2R. Wildtype (left, $n = 5$) and OX2R knockout mice (right, $n = 6$) were treated orally with vehicle (closed symbols, 20% Vit. E TPGS) and 100 mg/kg compound **5a** (open symbols) in a balanced cross-over paradigm. Dose time (arrow) occurred during the dark, or active phase 4 h prior to lights on (grey, white horizontal bars, bottom). Mean time in vigilance state during 30 min analysis intervals following vehicle and compound treatment conditions were compared using a linear mixed effects model for repeated measures *t*-test where significant responses are indicated with grey lines where tick marks indicate significance level (short, medium, long, $p < 0.05, 0.01, 0.001$).

absent in mice lacking OX_2 receptors which not only demonstrates that these effects of compound **5a** are mediated through orexin receptors, but is also consistent with OX_2R being the primary mediator of orexin-induced arousal.[23,24] Average plasma exposure in satellite animals was 60 ± 9 μM-h.

While acetylene **5a** was not an inhibitor of CYP3A4 as noted for **5m**, it proved to be a potent time-dependent 3A4 inhibitor (with an IC_{50} shift ratio >6.4). In fact, it was found that all acetylene containing compounds prepared in Table 1 are time dependent inhibitors highlighting a potential for drug–drug interactions. Accordingly, further activities involving acetylene linked orexin antagonists described herein were ceased.

In summary, the SAR of carbon replacements of the piperidine ether region of the DORA filorexant was reported. This region could be replaced with acetylene linkages as represented by **5a**, which was a potent DORA that showed pharmacological activity in a mouse sleep EEG model. While this structural change also led to undesirable time-dependent inhibition of CYP3A4 leading to a no go for this series, additional SAR evaluation of this region of the filorexant remains and will be reported in due course.

Acknowledgements

We thank Mr. Yunfu Luo (WuXi AppTec) for assistance in the preparation of intermediates 15 and 20.

References and notes

1. de Lecea, L.; Kilduff, T. S.; Peyron, C.; Gao, X. B.; Foye, P. E.; Danielson, P. E.; Fukuhara, C.; Battenberg, E. L. F.; Gautvik, V. T.; Bartlett, F. S.; Frankel, W. N.; van den Pol, A. N.; Bloom, F. E.; Gautvik, K. M.; Sutcliffe, J. G. *PNAS* **1998**, *95*, 322.
2. Sakurai, T.; Amemiya, A.; Ishii, M.; Matsuzaki, I.; Chemelli, R. M.; Tanaka, H.; Williams, S. C.; Richardson, J. A.; Kozlowski, G. P.; Wilson, S.; Arch, J. R. S.; Buckingham, R. E.; Haynes, A. C.; Carr, S. A.; Annan, R. S.; McNulty, D. E.; Liu, W. S.; Terrett, J. A.; Elshourbagy, N. A.; Bergsma, D. J.; Yanagisawa, M. *Cell* **1998**, *92*, 573.
3. Gotter, A. L.; Webber, A. L.; Coleman, P. J.; Renger, J. J.; Winrow, C. J. *Pharmacol. Rev.* **2012**, *64*, 389.
4. Grady, S. P.; Nishino, S.; Czeisler, C. A.; Hepner, D.; Scammell, T. E. *Sleep* **2006**, *29*, 295.
5. Taheri, S.; Sunter, D.; Dakin, C.; Moyes, S.; Seal, L.; Gardiner, J.; Rossi, M.; Ghatei, M.; Bloom, S. *Neurosci. Lett.* **2000**, *279*, 109.
6. Xie, X. M.; Wisor, J. P.; Hara, J.; Crowder, T. L.; LeWinter, R.; Khroyan, T. V.; Yamanaka, A.; Diano, S.; Horvath, T. L.; Sakurai, T.; Toll, L.; Kilduff, T. S. *J. Clin. Invest.* **2008**, *118*, 2471.
7. Bettica, P.; Squassante, L.; Zamuner, S.; Nucci, G.; Danker-Hopfe, H.; Ratti, E. *Sleep* **2012**, *35*, 1097.
8. Hoever, P.; de Haas, S. L.; Dorffner, G.; Chiossi, E.; van Gerven, J. M.; Dingemanse, J. *J. Psychopharmacol.* **2012**, *26*, 1071.
9. Herring, W. J.; Snyder, E.; Budd, K.; Hutzelmann, J.; Snavely, D.; Liu, K.; Lines, C.; Roth, T.; Michelson, D. *Neurology* **2012**, *79*, 2265.
10. Kuduk, S. D.; Winrow, C. J.; Coleman, P. J. *Annu. Rep. Med. Chem.* **2013**, *48*, 73.
11. Coleman, P. J.; Cox, C. D.; Roecker, A. J. *Curr. Top. Med. Chem.* **2011**, *11*, 696.
12. Rufoff, C.; Cao, M.; Guilleminault, C. *Curr. Pharm. Des.* **2011**, *17*, 1476.
13. Gotter, A. L.; Roecker, A. J.; Hargreaves, R.; Coleman, P. J.; Winrow, C. J.; Renger, J. J. *Prog. Brain Res.* **2012**, *198*, 163.
14. Mieda, M.; Sakurai, T. *CNS Drugs* **2013**, *27*, 83.
15. Coleman, P. J.; Schreier, J. D.; Cox, C. D.; Breslin, M. J.; Whitman, D. B.; Bogusky, M. J.; McGaughey, G. B.; Bednar, R. A.; Lemaire, W.; Doran, S. M.; Fox, S. V.; Garson, S. L.; Gotter, A. L.; Harrell, C. M.; Reiss, D. R.; Cabalu, T. D.; Cui, D.; Prueksaritanont, T.; Stevens, J.; Tannenbaum, P. L.; Ball, R. G.; Stellabott, J.; Young, S. D.; Hartman, G. D.; Winrow, C. J.; Renger, J. J. *Chem. Med. Chem.* **2012**, *7*, 415.
16. Cox, C. D.; Breslin, M. J.; McGaughey, G. B.; Whitman, D. B.; Schreier, J. D.; Bogusky, M. J.; Roecker, A. J.; Mercer, S. P.; Bednar, R. A.; Lemaire, W.; Bruno, J. G.; Reiss, D. R.; Harrell, C. M.; Murphy, K. L.; Garson, S. L.; Doran, S. M.; Koblan, K. S.; Prueksaritanont, T.; Anderson, W. B.; Tang, C.; Roller, S.; Cabalu, T. D.; Cui, D.; Ball, R. G.; Hartman, G. D.; Winrow, C. J.; Renger, J. J.; Coleman, P. J. *J. Med. Chem.* **2010**, *53*, 5320.
17. Müller, S.; Liepold, B.; Roth, G.; Bestmann, H. J. *Synlett* **1996**, 521.
18. Bergman, J. M.; Roecker, A. J.; Mercer, S. P.; Bednar, R. A.; Reiss, D. R.; Ransom, R. W.; Harrell, C. M.; Pettibone, D. J.; Lemaire, W.; Murphy, K. L.; Li, C.; Preuksaritanont, T.; Winrow, C. J.; Renger, J. J.; Koblan, K. S.; Hartman, G. D.; Coleman, P. J. *Bioorg. Med. Chem. Lett.* **2008**, *18*, 1425.
19. The high throughput (HT) HPLC log*D* (pH 7) value was determined on and Agilent 1200 HPLC/DAD system and ChemStation software, both from Agilent Technologies, USA. Separations are carried out on a Poroshell 120 EC-C18, 30 mm × 3.0 mm I.D., 2.7 μm, (Agilent Technologies, USA). The mobile phase consists of phosphate buffered saline at pH 7 (mobile phase A) and acetonitrile (mobile phase B). The chromatographic system is calibrated with a set of standards with published shake-flask log*D* values. Linear regression is used to determine the calibration line relating the retention time to log*D* for the calibration standards. This line is then used to determine the HT HPLC log*D* (pH 7) value of API from the measured retention time by the HPLC/DAD analysis of the API solution.
20. Hitchcock, S. A. *J. Med. Chem.* **2012**, *55*, 4877.
21. Brisbare-Roch, C.; Dingemanse, J.; Koberstein, R.; Hoever, P.; Aissaoui, H.; Flores, S.; Mueller, C.; Nayler, O.; van Gerven, J.; deHaas, S.; Hess, P.; Qiu, C.; Buchmann, S.; Scherz, M.; Weller, T.; Fischli, W.; Clozel, M.; Jenck, F. *Nat. Med.* **2007**, *13*, 150.
22. Winrow, C. J.; Gotter, A. L.; Cox, C. D.; Tannenbaum, P. L.; Garson, S. L.; Doran, S. M.; Breslin, M. J.; Schreier, J. D.; Fox, S. V.; Harrell, C. M.; Stevens, J.; Reiss, D. R.; Cui, D.; Coleman, P. J.; Renger, J. J. *Neuropharmacology* **2012**, *62*, 978.
23. Dugovic, C. I.; Shelton, J.; Sutton, S.; Yun, S.; Li, X.; Dvorak, C.; Carruthers, N.; Atack, J.; Lovenberg, T. *Sleep* **2008**, *31*, A33.
24. Morairty, S. R.; Revel, F. G.; Malherbe, P.; Moreau, J. L.; Valladao, D.; Wettstein, J. G.; Kilduff, T. S.; Borroni, E. *PLoS ONE* **2012**, *7*, 39131.